WAVELET PROCESSING OF ACOUSTIC EMISSION SIGNALS FROM SCRATCH TESTS ON NITRIDE COATINGS

Rosa Piotrkowski
Escuela de Ciencia y Tecnología, Universidad Nacional de San Martín, Argentina.
Antolino Gallego
Dpto. Física Aplicada, E. U. de Arquitectura Técnica, Universidad de Granada, España.
José E. Ruzzante
U.A. ENDE, Comisión Nacional de Energía Atómica, Buenos Aires, Argentina.
María T. García Hernández
Dpto. Física, Escuela Politécnica Superior, Universidad de Jaén, España.

Keywords: Acoustic Emission, coatings, scratch-tests, microfracture, Wavelet Transform.

ABSTRACT

Wavelet Transform was applied to Acoustic Emission (AE) signals from Scratch Tests (ST) on stainless steel samples with Cr and Ti nitride surface coatings obtained by PVD. The implementetion of the signal processing method was aimed at characterizing the coating failure stages and evaluating the quality of and the differences between both type of coatings. In previous work we had identified different zones along scratches both with Scanning Electron Microscopy and the directly measured AE parameters. The zones corresponded to transversal microfractures on the coating and/or deboding microfractures between the substrate (steel) and the coating. AE permitted an earlier detection, but with the traditional AE inspection the identification of the different zones was not sufficiently clear. This fact showed the necessity of more sophisticated signal processing. The WT, adequate to analize the essentialy non staionary AE signals, was applied in this paper and the different stages could be precisely delimited by a small number of adequate parameters. One of the best was the f_{MWP} , frequency at which the WT calculated mean power of signals takes its highest value, considering its evolution along the ST.

1. Introduction

Scratch Tests (ST), eventually supplied with AE detection, have shown their potential to evaluate the adherence of thin coatings on metallic substrates [1-2].

In a previous work, we studied AE signals from ST on stainless steel samples with Cr and Ti nitride coatings, in order to implement a signal processing method aimed at detecting the coating failure starting point [3]. ST were performed under controlled conditions with a device that consisted of a loaded probe with a diamond indenter moving linearly along the sample with a constant speed and continuously increasing force. The steadily increasing contact load causes tensile stress behind the indenter tip (trailing edge) and compressive stress ahead of the cutting tip (leading edge). The detection system used was MISTRAS 2001 from Physical Acoustics Corporation (PAC). The piezoelectric sensor was located with a coupling wax on the topside of the sample holder. Then signals passed through preamplifiers (40 dB) and were measured by the AEDSP-32/16B card that has two channels for signal processing and wave shape determination. The breakdown of the coatings was determined both by AE signal analysis and Optical and Scanning Electron Microscopy (OM and SEM), allowing to observe behavior differences between both kinds of coatings: CrN is fragile and TiN is ductile, appearing in both cases different zones of fracture. We have identified these zones by means of the analysis of the AE parameters (number of hits, energy, rise-time, duration). By performing SEM observations, the presence of different kind of microcracks could be assigned to each zone: transversal microcracks on the coating and/or deboding microcracks between the substrate (steel) and the coating. Thus, by using the traditional AE we could obtain interesting information about the material's fracture process. AE permits an earlier detection, because the shear stress is a maximum at certain depth from the surface, where a subsurface crack starts. In modern coatings, the first cracks are so small that they are difficult to perceive even under the microscope. They may even close-up within a few milliseconds and thus become optically "undetectable". Nevertheless, with the traditional AE inspection (without signal processing) we could not separate both kind of microcracks (deboding and transversal microcracks), so important information about the process was missing.

In the present paper, the WT, adequate to treat non-stationary signals, was applied, and different parameters coming from this processing method were investigated, in order to obtain a neat classification of stages, detecting in this way the debonding starting point.

2. The Wavelet Transform

One of the common techniques in spectral analysis of signals is the Fast Fourier Transform (FFT), which allows determining the frequency range that is predominant in a continuous signal. A continuous AE signal means that the time interval between emissions with similar amplitude is shorter than or equal to the emission duration. Therefore, the starting and ending points of events are not well defined. When signals are analyzed with the FFT, a local analysis is performed but when the temporal window is selected, an arbitrary and not always adequate frequency range is simultaneously defined. This is the reason why other transforms such as the Short Time Fourier Transform (STFT) and the Wavelet Transform were created. In the STFT the selection of the width of the temporal window is a non-trivial problem, in particular in cases where short and long time phenomena coexist. This is the case of our signals. Because AE is typically a non-stationary process, the Wavelet Transform is a useful tool to manage the data. It can be considered as the local Fourier Transform at all different scales [4]. WT was applied with good results in various papers of our Group, with different authors [5-7].

A wavelet $\psi(t)$ is an oscillating function of short duration, temporarily localized around the center $t = 1/2$. Its spectrum $|\hat{\psi}(\omega)|^2$ concentrates in a bilateral band $0 < \omega_1 \le |\omega| \le \omega_2$.

This mother function generates by means of dilatations and displacements a family of elemental functions or atoms, $\psi_{jk}(t)$ with localization in time – frequency, varying in an inverse proportion:

$$\psi_{jk}(t) = 2^{j/2}\psi(2^j t - k) \qquad j,k \in Z$$

By choosing properly the wavelet $\psi(t)$, the generated family constitutes an orthonormal basis of the space of signals with finite energy. So, given a signal *s(t)* , it is possible to represent it by the series:

$$s(t) = \sum_j \sum_k c_{jk}\psi_{jk}(t)$$

where

$$c_{jk} = \int_{-\infty}^{\infty} s(t)\,\psi_{jk}(t)\,dt \qquad (1)$$

These coefficients summarize without any redundancy the whole signal information. In addition, the energy relation holds:

$$\int_{-\infty}^{\infty} |s(t)|^2 dt = \sum_j \sum_k |c_{jk}|^2 \qquad (2)$$

The set of values (c_{jk}) constitutes the *Discrete Wavelet Transform* of the signal. Associated with the wavelet $\psi(t)$, there is the scaling function $\phi(t)$, centered in *t=0* and with spectrum $\left|\hat{\phi}(\omega)\right|^2$, concentrated in the low frequency band $|\omega| \le \omega_1$, which allows the alternative representation:

$$s(t) = 2^{-1/2}\sum_n s_{-1,n}\phi(\tfrac{t}{2}-n) + \sum_{j\le -1}\sum_k c_{jk}\,\psi_{jk}(t) = s_{-1}(t) + \sum_{j\le -1} q_j(t)$$

Each detail component $q_j(t)$ is related to a band of frequencies, that is,

$$\left[2^j\omega_1, 2^j\omega_2\right]$$

to a detail space W_j generated by the wavelets $\psi_{jk}(t)$. By means of an appropriate pair of discrete filters, h and g, it is possible to compute recursively the coefficients $s_{-1,n}$ and c_{jk} from the signal data $s_{0,n} = s(n\,\Delta t)$, with a sampling Δt. The mentioned discrete filters, h and g, are those which perform the recursive relations:

$$\begin{cases} \phi(t) = 2^{1/2}\sum_k h_k\phi(2t-k) \\ \psi(t) = 2^{1/2}\sum_k g_k\phi(2t-k) \end{cases}$$

In this paper, our calculations were mostly connected with energy of signals given by Equation (2). For the calculation of the coefficients, we employed the free software AGU-Vallen Wavelet (2002) specially developed for AE signals. In this case, the mother wavelet is a Gabor wavelet with a gaussian function.

The wavelet coefficients constitute a matrix with elements c_{ij}, corresponding the first subscript to the number of the frequency interval and the second one to the number of the time interval. If the addition on the second subindex of the squared coefficients is performed, the obtained parameter is named Wavelet Power (WP), that is:

$$WP_i = \frac{1}{N}\sum_j \left|c_{ij}\right|^2 \qquad (3)$$

Obviously, Equation (3) is a function of the frequency interval considered, where N is the number of wavelet coeficients for each i (frequency in our case). As we shall see in the next paragraph, another parameter will be very useful, f_{MWP}, defined as the frequency at which WP takes its maximum value for each signal.

3. Results and Discussion

In a previous work [3] we had presented AE results from ST with samples covered with TiN and CrN, which were characterized respectively as ductile and fragile. The description of the samples, elaboration process and the ST are in the quoted papers. In the present paper, the results refer to the same TiN sample (sample E) and the same ST (scratch 1). Summarizing previous results, and with the aim of comprehensibility, Figure (1) shows the SEM micrography of this scratch, in which a scale graduated in ten per cent indicates the position on the scratch (position %). Figure (2) shows Energy of each recorded hit versus Position % at which it was emitted, together with the corresponding applied load and Accumulated Energy. From Figures 1 and 2, four fracture zones were identified and are described in Table 1.

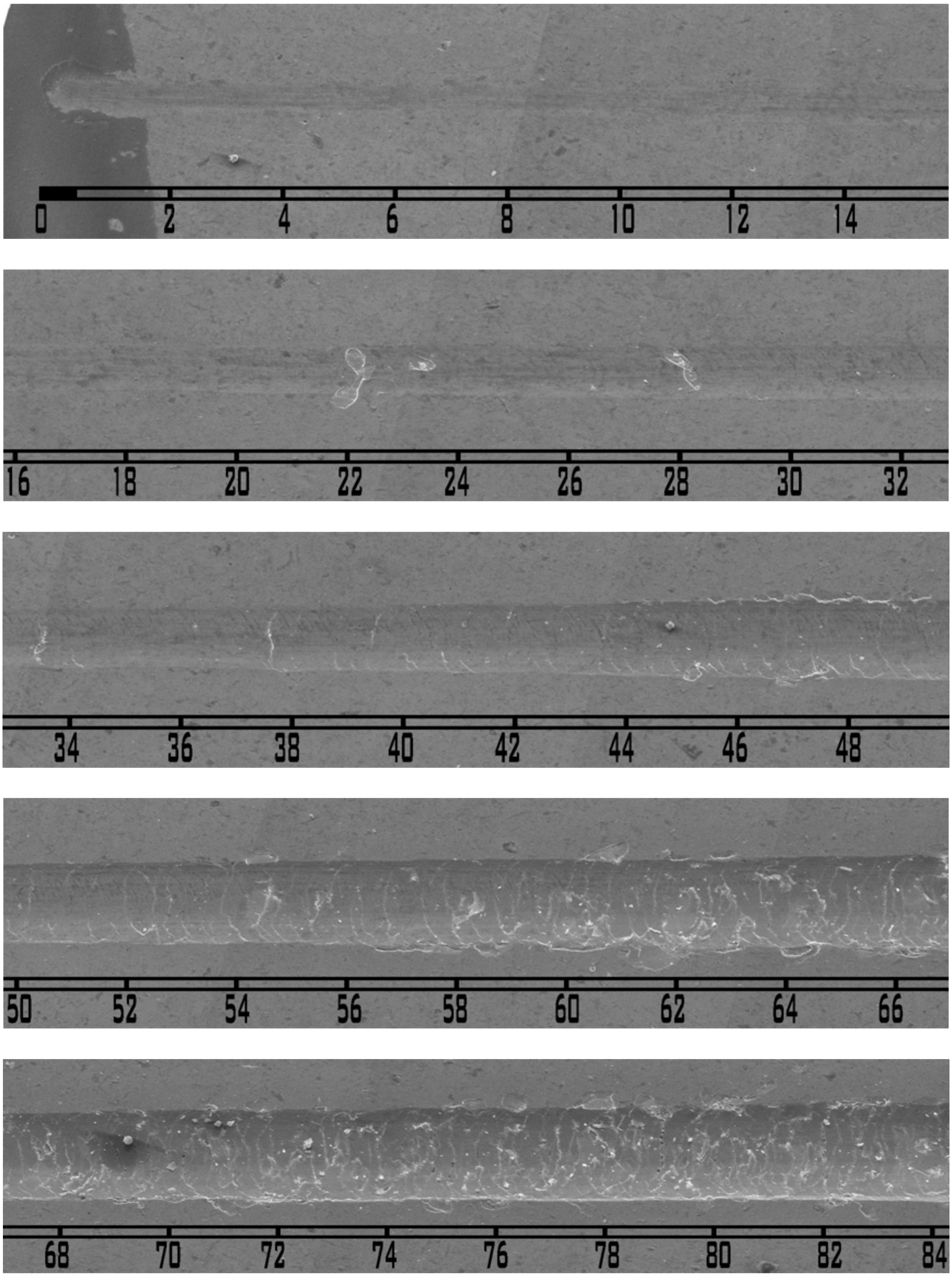

Figure 1.Scanning electron micrograph. Scratch 1, Sample E, TiN.

This analysis, in spite of being effective to characterize the different fracture zones has limitations:

- It does not permit the distinction of the two types of cracks in zones where they overlap.
- It does not remarkably predict the appearance of microscopic damage.

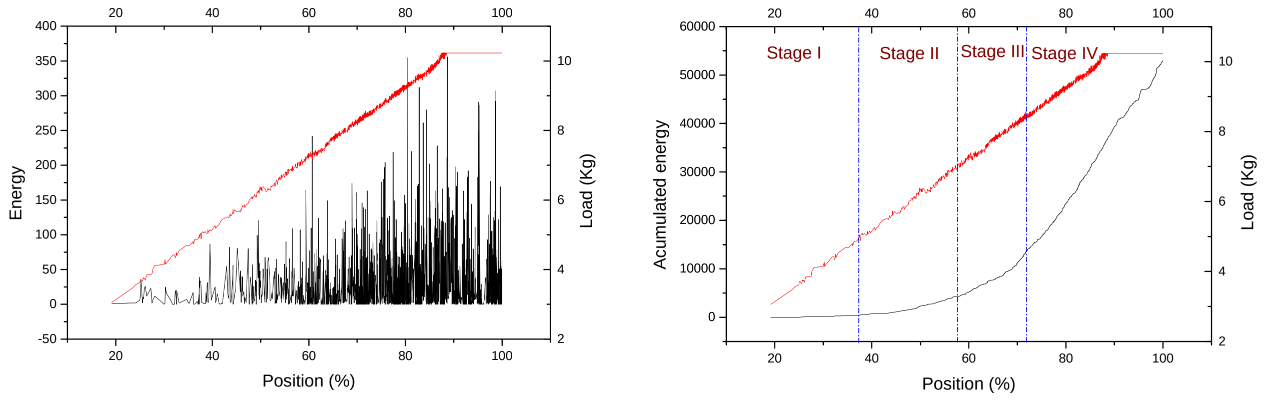

Figure 2. AE results for Scrath 1, Sample E (TiN). Left: Energy of hits and load vs. position %. Right: accumulated energy vs. position %.

Zone	**Position (%)**	**Description**	
		SEM	**AE**
I	0-37	Few transversal microcracks	Low accumulated energy (Slope 1)
II	37-58	Increasing number of transversal microcracks	Slight increase of accumulated energy (Slope 2)
III	58-72	Great number of transversal microcracks and a few number of debonding microcracks	Non-linear increase of accumulated energy (Change of Slope)
IV	72-100	Great number of both type of microcracks	Further increase of accumulated energy. (Slope 3)

Table 1. Comparison of the evolution of AE accumulated energy and presence of different type of microcracks along Scratch Test 1 in Sample E (TiN), as referred in [3].

For these reasons, we decided to perform further AE signal processing, like the WT employed in the present paper. We have calculated for each of the 641 signals corresponding to ST 1, sample E, the wavelet coefficients with the software Vallen (2000). The result was a matrix with elements c_{ij}, corresponding the first subscript to the number of the frequency interval and the second one to the number of the time interval. According to sampling frequency and duration of signals, frequency (f) ranged between $[0\text{-}1000]$ kHz, with $\Delta f=10$ kHz, and time (t) ranged between $[0\text{-}400]\mu$ s, with $\Delta t=0.4\mu$ s. With these coefficients we calculated the wavelet power for each frequency interval with Equation (3). The number of signal was uniformly displayed on a continuous axis, so that signal 641 corresponded to a position 100%. This result is shown in Figure 3.

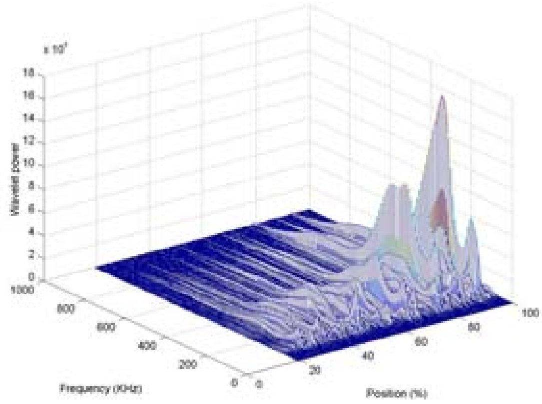

Figure 3. Wavelet power vs. frequency and position %. Scratch 1, Sample E (TiN).

In this Figure, it can be observed that important changes occur along the ST. For instance, while at the beginning high power values are at low frequencies, in the middle and at the end the higher values move to higher frequencies. This was the clue to find a very adequate parameter: frequency at which the wavelet power took its maximum value for each signal (position %). This parameter was named as f_{MWP}. This result is sown in Figure 4 versus the position (%).

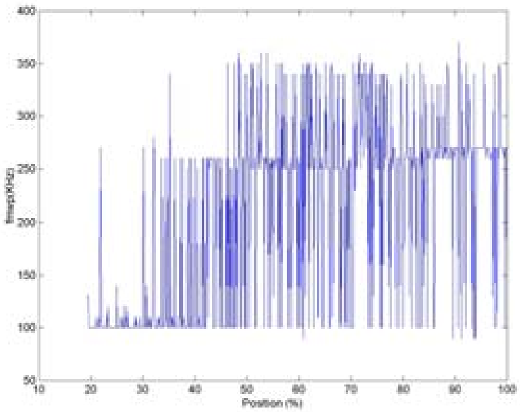

Figure 4. Frequency at which WP is a maximum (f_{MWP}) vs. position %. Scratch 1, Sample E (TiN).

Figure 4 shows 4 zones:

-Zone 1 (0-31%): Practically all f_{MWP} values of AE signals are low, around 125KHz.
-Zone 2 (31-46%): New intermediate f_{MWP} values appear around 250KHz.
-Zone 3 (46-70%): New high f_{MWP} values appear, around 350KHz.
-Zone 4 (70-100%): Idem Zone 3, but with a relatively higher number of signals with f_{MWP} around 350KHz.

In order to corroborate this result, three frequency bands were considered: [0-150] kHz, [150-275] kHz and [275-375] kHz. We calculated the WP corresponding to each band and divided this value by the total WP, corresponding to the whole [0-1000] kHz interval. In this way, we obtained the WP (%) contained in each band vs. position %, that is shown in Figure 5 and summarized in Figure 6. The left picture in Figure 5 corresponds to the band [0-150] kHz. We can see that between positions 0 and 31%, the higher powers take place for this band. In the middle picture in Figure 5, that corresponds to the band [150-275] kHz, the WP (%) is first low, and then it increases linearly between 31 and 46%. Finally, in the band [275-375] kHz high WP (%) values appear at 46 position % and increase linearly with position.

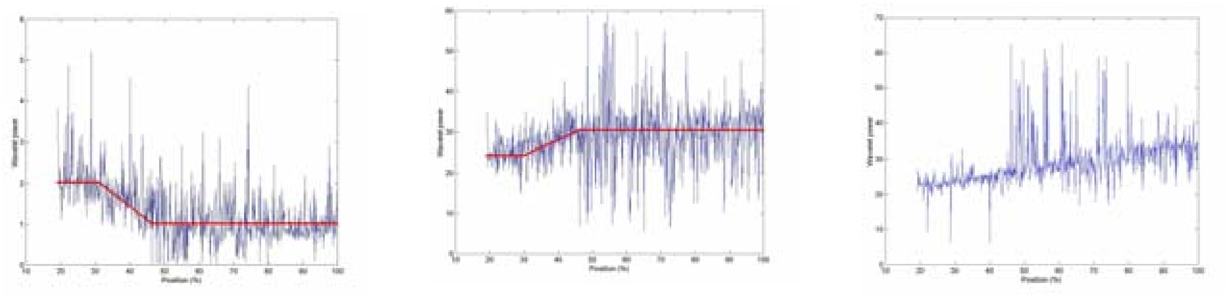

Figure 5. WP(%) vs. Position % for different frequency bands. Left: [0-150] kHz; Center: 150-275] kHz; Right: [275-375] kHz.

All these results, both the new ones corresponding to the present paper (Figures 3 and 6) and those previously obtainded (Figures 1 and 2 and Table 1), conduce to associate signals corresponding to the second band with transversal cracks, and signals corresponding to the third band with debonding cracks. Signals corresponding to transversal cracks are first detected at a position of ·31 % and are present till the end. Signals with f_{MWP} parameter in the third band can be connected with debonding cracks. They are significant from a position 46%, and suddenly increase at 70 %. Signals corresponding to the first band do not correspond to visible cracks in the SEM. They could correspond to crack nucleation and are present trough the whole ST.

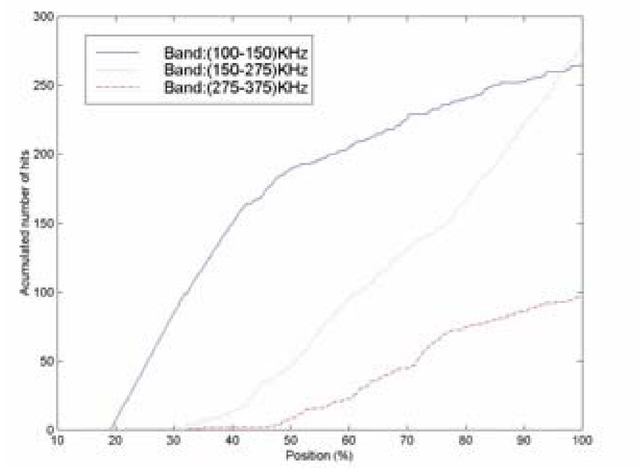

Figure 6. Accumulated number of hits vs. Position (%) for the different frequency bands.

With these criteria to classify AE signals based on the f_{MWP} , which can be associated with the microfracture process, signals of different types can be counted along the ST. This result is in Figure (6), which shows the evolution of the three type of signals. In this figure the initiation of zones 1, 2 and 3 is clearly seen. Also we can interpreted that at 70% an increase of the debonding cracks occurs and at 75% the same happens with the transversal craks, so, at 70% we can say that a fourth zone begins, in coincidence with the classification in Table (1). Moreover, it can be observed that the beginning of signals coming from debonding cracks at 46%, is preceded by a considerable increase of signals coming from transversal cracks at approximately 43%. This makes sense, because the transversal cracks could weaken the coating and favor in this way the onset of the debonding process.

With the present analysis, it was not only possible to clearly separate AE signals according their sources, but the limits of the different zones were also slightly modified, and in a sense that they precede the values obtained in previous work. So, the newly proposed method is a better predictor of the different fracture zones. In all cases it appears before visual damage and also before the plain traditional AE parameters.

4. Conclusions

A signal processing method based on the Wavelt Transform was applied to AE signals coming from ST on a TiN coating.

Results were compared with scanning electron microscopy observations, where different zones were identified along the scratch, according to type (transversal or debonding), and quantity of craks. Results were also compared with classification of zones according to previously obtained traditional AE parameters.

A very adequate AE parameter was found to better identify the onset of different fracture processes along the ST: it was the frequency at which the wavelet power took its maximum value for each signal of the ST. This parameter was named as f_{MWP}.

Different values of frequency interval for f_{MWP} could be associated with different type of cracks: [150-275] kHz to transversal cracks and [275-375] kHz to debonding cracks.

Four zones were determined along the ST. They were, measured in position %.: [0, 31], [31,46], [46,70] and [70,100]. The second zone began with the onset of transversal fracture of the coating, the third with the onset of deboding fracture of the coating, the fourth zone corresponded to a significant increase of both type of fracture. The first zone could not be associated with visible damage. It could be due to crack nucleation processes.

The present analysis provides more sensible tools and better predictors to identify different damaged zones in coatings tested with ST controlled by AE signals.

5. References

[1] Dalmas B.D., Benmedakhene S., Richard C., Laksimi A., Bégenger G. and Grégoire T., 2001, “Caractérisation par émission acoustique de l’adhérence et de l’endommagement d’un revetement: cas d’un revetement WC-Co sur acier”, C.R. Acad. Sci. Paris, Chimie/Chemistry, Vol. 4, pp. 345-350.

[2] Piotrkowski R., Hirchoren G.A., Gómez M.P, D'Attellis C.E and Ruzzante J.E., 1999, "Acoustic emission signals from a coating breakdown, 1/f processes and wavelet analysis", Proceedings of the First Meeting of the Acoustic Emission Latin-American Group, E-GLEA 1, Buenos Aires, 6-10 September, pp. 177-188.

[3] Piotrkowski R., Gallego A., Ruzzante J.E., García-Hernández M.T., 2002, “Adherence of nitride coatings analyzed by acoustic emission signals coming from Scratch tests”, The eJournal of Nondestructive Testing & Ultrasonics, ISSN: 1435-4934.

[4] Chui C.K., 1992, “An Introduction to Wavelets”, Academic Press, San Diego, USA.

[5] Maradei C. Piotrkowski R., Serrano E., 2002, Ruzzante J.E., “Monitoring of the tool condition with acoustic emission signal analysis using wavelet packets”, Insight, Vol. 44, No. 12, pp. 786-791.

[6]Vargas G., Isaacson S.I., D'Attellis C.E., López Pumarega M.I., Ruzzante J.E., Piotrkowski R., 2000, "Automatic analysis of acoustic emission signals", 15th World Conference on Non-Destructive Testing, Roma, 15-21 October, IDN:.483

[7] Ruzzante J.E., Serrano E.P., 2000, “Estimation of differences in event arrival times with Wavelet Transform techniques” 15th World Conference on Non-Destructive Testing, Roma, 15-21 October, IDN: 445.